SIMULATION OF A NOVEL PHOTONIC TRANSMISSION SYSTEM USING M-ary AMPLITUDE-PHASE DIFFERENTIAL SHIFT KEYING MODULATION FORMAT

Tran. D. Dung, Huynh. T. Liem, Le. N. Binh
Department of Electrical and Computer Systems Engineering, Monash University, Clayton, Victoria 3800, Australia
Correspondence Email: le.nguyen.binh@ eng.monash.edu.au

ABSTRACT

We propose a photonic transmission system based on 16-ary multi-level amplitude-differential phase shift keying (MADPSK) format and its generation using a dual-drive interferometric electro-optic modulator. The modulation scheme is bandwidth efficient with an effective transmission symbol rate equal to ¼ of the bit rate. The transmitter requires only a single modulator to give amplitude and phase modulations. Simulation models are developed for evaluation of the system transmission performance. The multi-level optical signal spectra, eye diagrams and bit-error-rates are obtained to demonstrate the lightwave-modulated multi-level scheme transmission over the dispersive single mode optical fibres.

1. INTRODUCTION

Over the last few years, due to the increasing demand of broadband services, the necessity of upgrading the current Dense Wavelength Division Multiplexed (DWDM) 10Gb/s/channel systems to DWDM 40 Gb/s/channel becomes more and more crucial. Recently several modulation techniques based on differential phase modulation and detection such as binary differential phase shift keying (BDPSK), differential quadrature PSK (DQPSK) have attracted significant interest as alternatives for conventional on-off keying (OOK or amplitude shift keying - ASK). However, in these schemes the number of levels encoded in a signal symbol falls far behind 256 or 1024 achieved in their microwave modulation counterparts [1]. This is due to the phase noises associated with optical sources and optical amplifiers (OAs) employed along the transmission in-line fibres. Furthermore the demands of upgrading the transmission capacity over currently installed optical fibres require bandwidth effective modulation schemes for long haul optically amplified transmission.

One possibility for increasing the channel capacity is to employ multi-level modulation scheme, hence the symbol rate can be reduced proportionally to $\log_2 M$, where M is number of signal levels. In this paper, in order to significantly increase the number of levels, hence, obtaining spectral efficiency, we propose the use of DQPSK in combination with ASK to create multi-level amplitude-differential phase shift keying (MADPSK) signal. Thus, we employ a hybrid modulation scheme taking advantage of the amplitude and phase modulation techniques that have been well developed over the last decade. The differential scheme is used so as to minimize the demand on the coherence of the lightwave sources. That is, the coherence of the source is required only for the duration of the two consecutive bit periods. A MADPSK signal can be generated by a number of discrete phase and amplitude modulators in cascade [1], [2]. In this paper, we also report a simpler and more efficient alternating technique for generating MADPSK signals using only a single dual-drive electro-optic Mach-Zehnder interferometric modulator (MZIM).

The paper is organized as follows: Section 2 describes a method of generating MADPSK signal using dual-drive MZIM. In Section 3, we propose and report the development of a novel photonic transmission system based on MADPSK modulation format. Section 4 illustrates the transmission performance including the phasor scattering property, the eye diagrams and the Q-factor versus the bit-error rate.

2. THE DUAL-DRIVE MZIM AND MADPSK SIGNAL GENERATION

The constellation of 16-ary MADPSK signal is shown in Fig. 1. It is similar to that used in [1] and indeed, a combination of 4-ary ASK and DQPSK schemes. The four bits [D_3, D_2, D_1, D_0] are mapped into a symbol, among them two bits [D_1D_0] are coded into four phases [$0, \pi/2, \pi, 3\pi/2$] and two bits [D_3D_2] are coded to create four amplitude levels. As demonstrated in [1], with the use of a balanced optical receiver and a photonic delay interferometer (DI), the MADPSK scheme produces a clear DQPSK eye opening centered at zero-voltage decision level only when constellation points are positioned in a radial pattern as shown in Fig. 1.

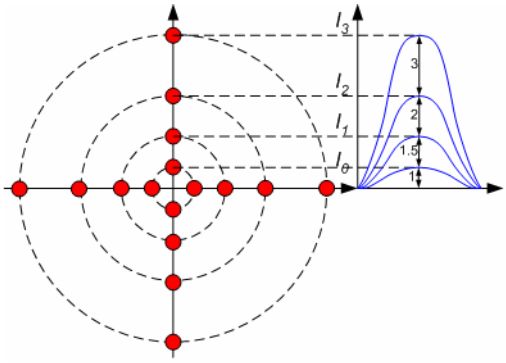

Fig. 1. In-phase and quadrature ASK and PSK inter-level signal-space and intensity detected signal levels.

A dual-drive MZIM has two driving voltages that independently modulate the phases of the lightwave carriers passing the top and the bottom waveguide branches as shown in Fig. 2. When the phase shifts applied to the branches are electrically in phase, the interference at the output of the dual-drive MZIM produces phase modulated lightwave. However, when the phase shifts in the two branches are exactly equal but opposite in sign the output signal is intensity modulated. Thus the dual-drive MZIM can be used for both phase and intensity modulation simultaneously. That means that to generate a MADPSK signal using the dual-drive MZIM, it is not necessary to employ separate phase and amplitude modulators as reported in [1] and [2].

The relationship between signals at the input and output fields E_{output} and E_{input} of the dual-drive MZIM is [3] :

$$E_{output} = \frac{E_{input}}{2}\left[\exp\left(j\pi\frac{V_1(t)}{V_\pi}\right)+\exp\left(j\pi\frac{V_2(t)}{V_\pi}\right)\right] \quad (1)$$

where $V_1(t)$ and $V_2(t)$ are the time dependent driving voltages (bias DC voltages included) applied to the electrodes, V_π is the voltage required to provide a π phase shift of the carrier in each branch of MZIM.

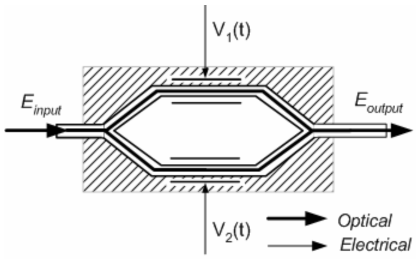

Fig. 2. Schematic diagram of an electro-optic dual-drive MZIM, the applied voltages $V_1(t)$ and $V_2(t)$ are superimposed by a DC bias voltage and a time-variant signals coupled via a microwave bias-T components.

Eq. (1) suggests that with an appropriately chosen input signal E_{input} and driving voltages $V_1(t)$, $V_2(t)$, all signal points of the constellation can be constructed from two signal phasors $\frac{E_{input}}{2}e^{j\phi_1}$ and $\frac{E_{input}}{2}e^{j\phi_2}$. Indeed, if E_{input} is chosen to be equal the electrical field corresponding to the signal points in the largest circle of the constellation, then a signal point E_{output} with the phase shift θ_i in the circle n can be found as a sum of two vectors $\frac{E_{input}}{2}e^{j\phi_{ni1}}$ and $\frac{E_{input}}{2}e^{j\phi_{ni2}}$, where:

$$\phi_{ni2} = \theta_i - \arccos\left(E_n / E_{input}\right),\ \phi_{ni1} = \theta_i + \arccos\left(E_n / E_{input}\right) \quad (2)$$

The subscrips i and n denote the phase position and the order of the circle of interest respectively.

Fig.3 illustrates the relationship between E_i, E_0, ϕ_{ni1} and ϕ_{ni2}. For the sake of simplicity the signal point is chosen with $\theta_i = 0$. Hence by substituting ϕ_{ni1} and ϕ_{ni2} into (2) we obtain the driving voltages for this signal point:

$$V_{ni1} = \frac{V_\pi}{\pi}\left[\theta_i + \arccos\left(E_n / E_i\right)\right],\ V_{ni2} = \frac{V_\pi}{\pi}\left[\theta_i - \arccos\left(E_n / E_i\right)\right] \quad (3)$$

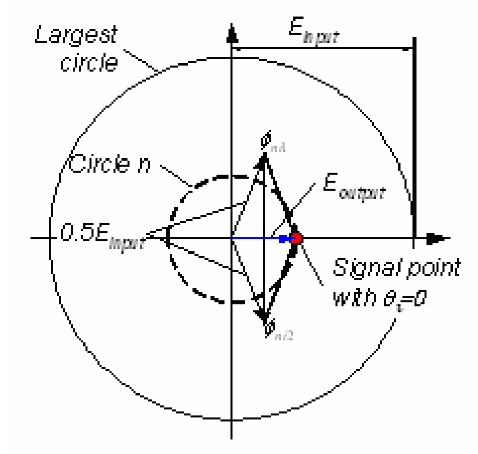

Fig. 3. Illustration of the relationship between E_{input}, E_{output}, ϕ_{ni1} and ϕ_{ni2} in a phasor signal-space.

Therefore the multi-level amplitude signal-space shown in Fig. 1 can also be generated using the same MZIM by driving the two traveling wave electrodes of the modulator with different amplitudes. The phase generation of each signal space circle can be integrated by an appropriate assignment of the voltage levels.

3. PROPOSED M-ARY AMPLITUDE-PHASE PHOTONIC MODULATION

3.1. Signal model

The signal model described in Section 2 is used. To balance the ASK and DQPSK sensitivities, the ASK signal levels are preliminary adjusted as shown in Fig. 1 to the ratio $[I_3 / I_2 / I_1 / I_0] = [3/2/1.5/1]$ [1][4]

3.2. System simulation

An optical simulation model has been developed to demonstrate the photonic transmission system and for evaluation of its transmission performance. It consists of transmitter, receiver, and propagation fiber models.

The transmitter shown in Fig. 4 (b) and (c) is used to produce 16-ary MADPSK signal. It consists of a DFB laser source generating the lightwave carrier that can then externally modulated in both phase and amplitude via the dual-drive MZIM. Each bit of the four bit symbol of the user data [$D_3D_2D_1D_0$] is first grouped, then pre-encoded to generate two electrical driving signals $V_1(t)$ and $V_2(t)$. The amplitude and phase of the lightwave carrier propagating through the two optical paths of the dual-drive MZIM are modulated to produce NRZ 16-ary MADPSK signal. Optionally, an optical pulse carver, RZM-PC, can be used to convert NRZ pulse train into RZ for improving sensitivity and minimizing frequency chirp.

The SimuLink model of this transmitter is shown in Fig. 4 consisting of (i) A “User data and ADPSK pre-coder” block generating pseudo-random data sequence to simulate user data stream and encodes each group of 4 data bits into a symbol; (ii) A “Voltage driver 1” and “Voltage driver 2” blocks mapping pre-encoded data to driving voltages for modulating amplitude and phase of the carrier in the dual-drive MZIM; (iii) Two “Complex phase shift” blocks representing two optical paths of the dual-drive MZIM; (iv) “Sum block” simulates the combiner at the output of MZIM; (v) A “Gaussian noise generator” block representing the noise source; and (vi) An “Amplifier” block that represents the optical amplification.

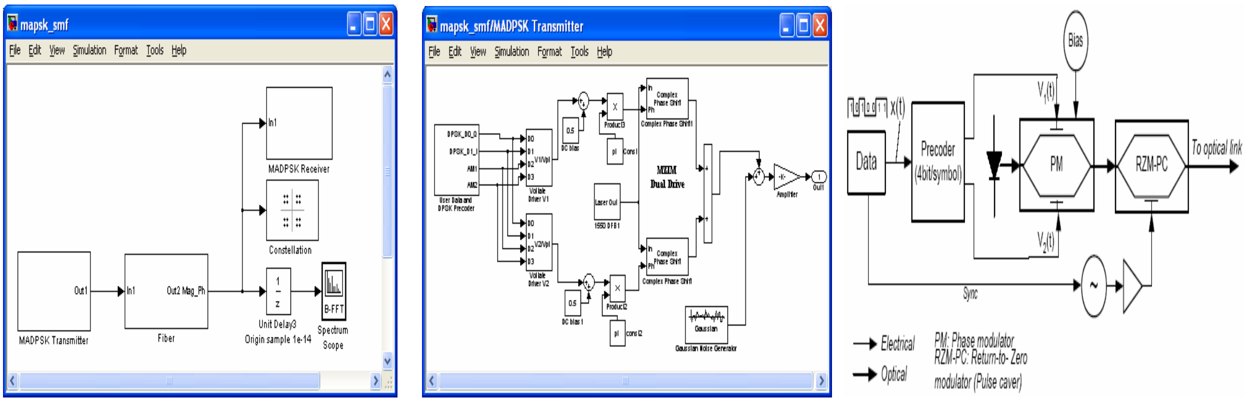

(a) (b) (c)

Fig. 4. (a) Models of the transmission system arrangement (b) the MADPSK transmitter and (c) implementation using external modulators.

3.3. Receiver Model

The balanced receiver, shown in Fig. 5(a), consists of two photonic DIs incorporating orthogonal optical phase shifters $\pi/4$ and $-\pi/4$, an amplitude demodulator, and a data multiplexer MUX. The two phase demodulators are used for extracting $[D_1D_0]$ bits while the amplitude demodulator (AD) is used to detect the amplitude of MADPSK signal to recover bits $[D_3D_2]$. They are then interleaved with the two bits $[D_1D_0]$ by the MUX to reconstruct the original binary data stream.

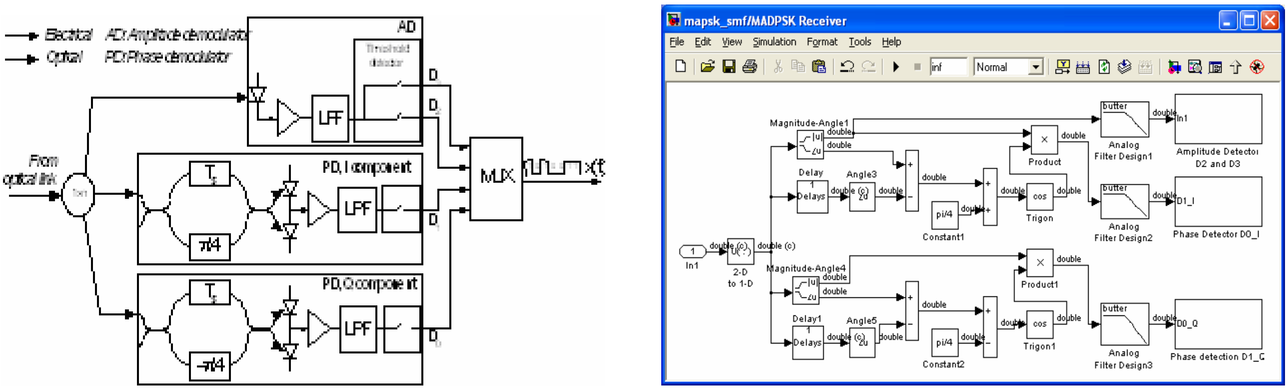

(a) (b)

Fig. 5. MADPSK receiver (a) hardware implementation (b) simulation model

The simulation model of the receiver is shown in Fig. 5(b) consisting of (i) two delay interferometers, each is simulated by a set of two "Magnitude-Angle" blocks, a "Delay block", and a "Sum" block. The "Delay block" stores the phase of the previous symbol, the "Magnitude-Angle" blocks extract the phase and amplitude of present and previous symbols, which will be used in different phase demodulation and detection operations; (ii) "Constant *pi/4*" and "Constant *-pi/4*" and next two "Sum" blocks simulate extra phase delay in each branch of DI; (iii) The "cos" and "product" blocks simulating the two balanced receivers (iv) "Amplitude Detector D2 and D3" block simulates ASK detector for D_2 and D_3 bits; (v) Three "Analog Filter Design" blocks simulate electrical low pass filters ; (vi) "Phase Detector D0_I" and "Phase Detector D1_Q" blocks simulate the threshold detectors for D_0 and D_1 bits (I and Q component of a DQPSK signal), respectively.

3.4. Transmission and Dispersion Compensating Fibres

The propagation evolution of the complex envelope *A(z,t)* of optical electric field signals along a nonlinear optical fiber is governed by the well-known nonlinear Schroedinger equation (NLSE) [5] :

$$\frac{\partial A(z,t)}{\partial z} + \frac{\alpha}{2} A(z,t) - \frac{j}{2}\beta_2 \frac{\partial^2 A(z,t)}{\partial t^2} - \frac{1}{6}\beta_3 \frac{\partial^3 A(z,t)}{\partial t^3} = -j\gamma \left|A(z,t)\right|^2 A(z,t) \quad (4)$$

where z is the spatial longitudinal coordinate, α accounts for fiber attenuation, β_2 and β_3 represent fibre dispersion and γ is the nonlinear coefficient. Equation (4) includes chromatic dispersion, high-order dispersion, attenuation and the nonlinear SPM phase effects of a single-channel propagation along an single mode fiber. The symmetric split-step-Fourier method (SSMF) is utilized and optimized to simulate the propagation of the lightwave modulated signals. The symmetrized SSFM can be optimized by: (i) split-step length that satisfies the constraint for the convergence; (ii) evaluation of incident peak power. If it is lower than the threshold of nonlinearities of the transmission fibre, the SPM effect can be neglected and SSFM will be switched to the Low Pass Transfer Function (LPTF) method that involves only the fibre dispersion and attenuation effects. The LPTF of the fibre is given as [5]:

$$H_f(f) = \exp\left\{-j\left[(1/2)\beta_2^{'}\varpi^2 + (1/6)\beta_3^{'}\varpi^3\right]L\right. \quad (5)$$

where $\varpi = 2\pi f$, L is length of transmission and

$$\beta_2^{'} \cong -\frac{\lambda^2}{2\pi c}D \quad (6)$$

$$\beta_3^{'} \cong \left(\frac{\lambda}{2\pi c}\right)^2\left(2\lambda D + D'\lambda^2\right) \quad (7)$$

with D is the fibre chromatic dispersion parameter at λ .

The dispersion compensation fiber model has the same structure of the propagation fiber model, except for the sign of the propagation constant *beta2* is opposite to that of *beta2* in the propagation fiber.

4. SIMULATION RESULTS

4.1. Signal Spectrum, Signal Constellation and Eye Diagram

The simulation spectrum of 40Gbps 16-ary MADPSK signal is given in Fig. 6(a). As it has been seen clearly in the graph, the single-sided bandwidth of the main lobe equals 10GHz. Numerically, it amounts to only a quarter of the transmission bit rate, and from that we conclude that MADPSK is a highly bandwidth efficient modulation format. Fig. 6(b) shows the signal constellation recovered at the receiving end. Amplifier noise and nonlinear property of fiber cause amplitude and phase fluctuations and scatter signal points. The simulated MADPSK eye diagram is shown in Fig. 6(c) for the I component. Similar eye diagrams are also obtained for the Q component. These eye diagrams clearly show four amplitude levels associated with two phase shifts 0 and π .

The average optical signal level of the outermost constellation has been assigned below the nonlinear self-phase modulation level of a standard single mode fibre, approximately about 2.6 mW. The signal-space constellation shown in Fig. 6(b) indicates that there are phase mismatching between the transmission and compensating fibres. We note also that the phase rotation is not uniform for the in-phase and quadrature components. The spectrum of the lightwave modulated MAPSK signals shows that the effective 3dB bandwidth is about 10 GHz, thus its is approximately equivalent to a 10Gb/s NRZ on-off-keying modulation format signals.

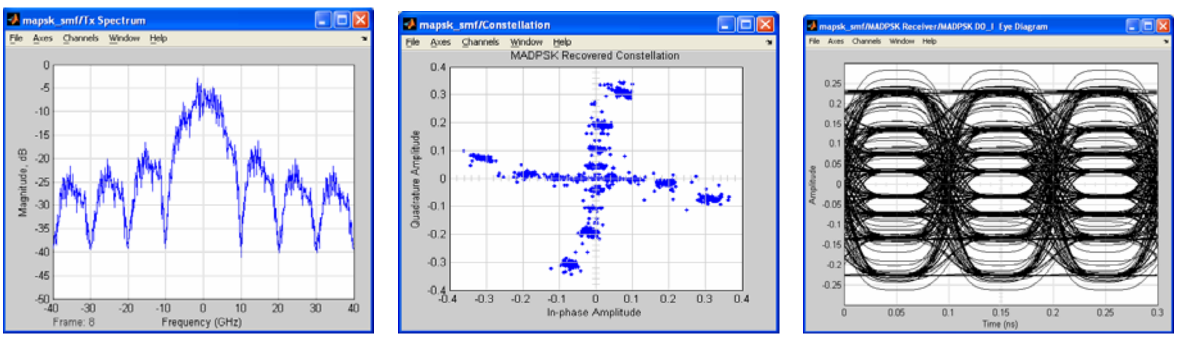

(a) (b) (c)

Fig. 6. (a) 40Gbit/s MADPSK spectrum before transmission (b). 40Gbit/s MADPSK constellation with dispersion compensation after 80 km standard SMF transmission (c). 40Gbit/s MADPSK eye diagram at OSNR=20dB.

4.2. System Performance Evaluation

The MADPSK system can be considered as consisting of two sub-systems, ASK and DQPSK and its error probability can be evaluated as join error probabilities of the two:

$$P_{ADPSK} = \left[\frac{1}{2}P_{ASK} + \frac{1}{2}P_{DPSK} - \frac{1}{2}P_{ASK} \cdot \frac{1}{2}P_{DPSK}\right] = \frac{1}{2}\left[P_{ASK} + P_{DPSK} - \frac{1}{4}P_{ASK} \cdot P_{DPSK}\right] \quad (8)$$

where P_{ASK} and P_{DPSK} are error probabilities of ASK and DQPSK sub-systems, respectively. We have assumed that these probabilities are evaluated independently with respect to each other. Fig. 7 shows the graphs of error probability for the ASK sub-system, DQPSK sub-system and MADPSK system in the same co-ordinates for comparison purpose.

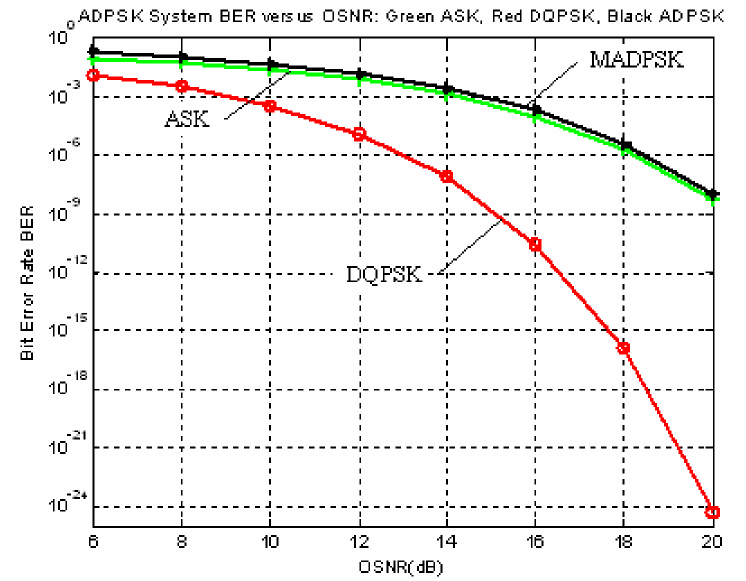

Fig. 7. Error probability of MADPSK (black) system versus OSNR. Error probability of ASK (green and overlapped) and MADPSK are nearly coincided.

At OSNR=20dB and bandwidth of 40MHz the system BER $\approx 10^{-9}$, that adequately meets the performance requirement for long haul transmission. It is also clear that for the same value of OSNR, especially when it is high, the DQPSK sub-system outperforms ASK counterpart, and the overall performance of MADPSK system are dominated by the ASK sub-system performance. Thus, we believe that with optimized ASK signal levels to balance between ASK and DPSK performance, the BER can be significantly enhanced. The simulated Q-factor and the BER indicate similar as obtained in Fig. 7.

5. CONCLUDING REMARKS

Current advanced photonic technology has enabled the use of differential phase modulation and demodulation in optical domain. Our proposed MADPSK modulation format combining ASK and DPSK modulation formats would offer a much higher bit rate than BDPSK and DQPSK formats. In another word for the same effective signal bandwidth the channel capacity is M-times higher. Consequently these amplitude-phase hybrid schemes offer higher spectral efficiency and hence allowing upgrading of the 10 Gb/s or 40Gb/s dense wavelength multiplexed optical transmission to 40 Gb/s and 160 Gb/s respectively. We have demonstrated experimentally the transmission of 40 Gb/s using DPSK and DQPSK schemes [7]. The demonstration of our proposed M-ary ADPSK would be reported in the near future. The noises of the optical amplifiers have not been considered in this report. We currently develop these models and incorporate with the transmission and dispersion compensating fibres for multi-span ultra-high capacity transmission.

Other signal-space constellation of the M-ary hybrid amplitude-phase differential shift keying modulation formats such as the offset constellation, the alternating amplitude-phase offset and equivalent quadrature amplitude modulation are under our current studies and will be reported in the future.

6. REFERENCES

[1] K. Sekine, et al., "40 Gbit/s 16-ary (4 bit/symbol) optical modulation/demodulation scheme", Elect. Lett., vol. 41, No. 7, March 2005.

[2] Hayase, S., et al., "Proposal of 8-state per symbol (binary ASK and QPSK) 30-Gbit/ optical modulation scheme". Proc. European Conf. on Optical Communication, ECOC 2003, Rimini, Italy, Sept. 2003, Paper Th2.6.4, pp. 1008–1009

[3] K-P. Ho, "Generation of Arbitrary Quadrature Signals Using One Dual-Drive Modulator", IEEE *J. Lightw. Tech,* Vol. 23, No. 2, pp. 764-770, Feb. 2005.

[4] Tran, D.D., Binh. L.N., Huynh, T.L. and Tiong, H.S., "Geometrical and Phasor Representation of Multi-level Amplitude-Phase Modulation Formats and Photonic Transmitter Structures", Proc. IEEE Tencon2005, Nov 2005, Melbourne, Australia.

[5] G.P. Agrawal, Nonlinear Fiber Optics, 3rd Ed., Academic Press, 2001.

[6] G.P. Agrawal, Fiber-optic communication systems, 3rd Ed. Academic Press, 2001.

[7] L.N. Binh, H.Q. Lam, T.L. Huynh and D.D. Tran, "Phase and Amplitude Modulation Formats for Hybrid 40 Gb/s 10Gb/s DWDM Photonic Long-Haul Transmission", submitted to WARS2006, Feb 2006, Leura, NSW, Australia.